LBL-31008

Lawrence Berkeley Laboratory

UNIVERSITY OF CALIFORNIA

Materials & Chemical Sciences Division

Presented at the 7th International Conference on
Surface Modification of Metals by Ion Beams,
Washington D.C., July 15–19, 1991,
and to be published in the Proceedings

Distribution of Ion-Implanted Yttrium in Cr_2O_3 Scale and in the Underlying Ni-25wt%Cr Alloy

P.Y. Hou, V. Chia, and I. Brown

July 1991

LOAN COPY
Circulates
for 4 weeks
Bldg. 50 Library.
LBL-31008
Copy 2

Prepared for the U.S. Department of Energy under Contract Number DE-AC03-76SF00098

DISCLAIMER

This document was prepared as an account of work sponsored by the United States Government. While this document is believed to contain correct information, neither the United States Government nor any agency thereof, nor the Regents of the University of California, nor any of their employees, makes any warranty, express or implied, or assumes any legal responsibility for the accuracy, completeness, or usefulness of any information, apparatus, product, or process disclosed, or represents that its use would not infringe privately owned rights. Reference herein to any specific commercial product, process, or service by its trade name, trademark, manufacturer, or otherwise, does not necessarily constitute or imply its endorsement, recommendation, or favoring by the United States Government or any agency thereof, or the Regents of the University of California. The views and opinions of authors expressed herein do not necessarily state or reflect those of the United States Government or any agency thereof or the Regents of the University of California.

Distribution of Ion-implanted Yttrium in Cr_2O_3 Scale and in the Underlying Ni-25wt%Cr Alloy*

P. Y. Hou[1] *Victor Chia*[2] *and Ian Brown*[1]

[1]Lawrence Berkeley Laboratory
1 Cyclotron Rd.
Berkeley, CA 94720

[2]Charles Evans and Associates
301 Chesapeake Dr.
Redwood City, CA 94063

ABSTRACT

Implantation of yttrium and other reactive metals has been known to show significant effects on the oxidation behavior of Cr_2O_3-forming alloys. The oxide growth rate decreases by nearly a factor of ten, and the adhesion of oxide scales to alloys is greatly improved. To better understand the mechanisms by which these elements affect oxidation, it is important to know whether or not they are present in the metal ahead of the oxide layer. In this study, the diffusivity of implanted yttrium in a Ni-25wt%Cr alloy and its distribution in the oxide scale after different oxidation times have been evaluated using secondary ion mass spectroscopy. It was found that only 17 ppm of yttrium was left in the alloy after just 20 minutes of oxidation at 1000°C. The implanted Y remained concentrated at the oxide/gas interface as the oxide thickened with time. Within the oxide layer, the Y concentration progressively dropped to zero at the scale/alloy interface. These results are discussed in relation to several important mechanisms proposed for the beneficial effects of reactive element additions on scale adhesion.

*This work was supported by the Electric Power Research Institute under contract No. RP 2261-1, through an agreement with the U. S. Department of Energy under Contract No. DE-AC03-76SF00098.

INTRODUCTION

All metallic components operating at elevated temperatures need the protection of a slow growing and adherent oxide scale, or a coating which can easily develop such a scale, to resist oxidation. The most common protective oxides in practice are Al_2O_3 and Cr_2O_3. It was discovered over 50 years ago[1] that minor additions of rare earth elements, less than 0.2 wt%, in these Al_2O_3- or Cr_2O_3-forming alloys greatly improved their oxidation resistance. Later it was established[2] that any elements which have a higher affinity for oxygen than the scale-forming element can be effective. For Cr_2O_3-forming alloys, the effects are: i) an enhanced selective oxidation of chromium by either lowering the amount of Cr required to form a continuous protective Cr_2O_3 layer, or by reducing the formation of base metal containing oxides in the external scale; ii) a reduction in the growth rate of the chromia scale, particularly at temperatures above 900°C; iii) a change in transport mechanism through the scale from principally metal transport outward for alloys without the reactive element addition to principally oxygen transport inward and iv) an increase in the resistance of the scale to exfoliation on either thermal cycling or mechanical straining.

Although the benefits of the reactive element addition have been put to practical use for many years, mechanisms which lead to these phenomena are still under much debate. In recent years, ion-implantation[3-5] has been a technique widely used for the study of these effects. Up to a critical dosage of about 1×10^{16} ions/cm^2[6-8], the implanted reactive elements exhibit the same effects as with alloying additions. The implanted element is found to be concentrated at the outer surface of the oxide scale. As the scale thickens with time, it remains concentrated at that location while the scale/alloy interface retreats inward[7,8]. The presence of these reactive elements within the growing oxide scale has been suggested to be the cause for the observed reduction in oxide growth rate and the modified growth mechanism[9,10], but it is still unclear as to how the scale adhesion can be improved.

Numerous mechanisms have been proposed to explain the role of the reactive elements in improving scale adhesion. Several of them however, require the reactive elements to be present in the alloy to either act as a sink for vacancies generated during oxidation which would otherwise condense at the interface to form voids[2], getter impurities, particularly sulfur, from the bulk of the alloy to segregate to the interface to weaken it[11], or provide fast diffusion paths for Cr to develop pegs of oxide which intrude into the metal to form an irregular but stronger interface. Since ion-implantation of reactive elements shows the same effects as their alloying additions, it is then important to know whether or not the implanted element is present in the alloy after oxidation. Such knowledge will greatly help in elucidating the mechanism by which the reactive element addition improves scale adhesion. Collins et. al.[12] found in oxidation of Y-implanted Cr that after removal of the oxide layer by polishing, the Cr sample still continued to exhibit reduced oxidation rate. This implies that some Y was left in the alloy after polishing, and the authors suggested that the Y had back-diffused into the alloy during oxidation. Those experiments however, were carried out only at 600°C where the oxidation rate of Cr is very slow and the effects of reactive element additions are usually not pronounced. The purpose of this study then is to determine if any of the ion-implanted yttrium is still present in a Ni-25wt%Cr alloy after its oxidation at 1000°C.

EXPERIMENTAL METHOD

The Ni-25wt%Cr alloy was prepared by induction melting and casting under an argon atmosphere, followed by a vacuum homogenization for 24 hours at 1100°C. The actual composition of Cr is very close to the nominal 25wt%. The alloy was found to contain 80 ppm of sulfur by weight. The average grain size was 1.5 mm x 0.4 mm x 0.3 mm. Specimens 15mm x 10mm x 1mm were cut from the center of the homogenized ingot, followed by a light grinding of all faces on SiC paper. One main face in particular was polished to a 1 μm finish with diamond paste for subsequent ion-implantation and oxidation studies.

Ion-implantation was carried out using a metal vapor vacuum arc (Mevva) high current metal ion implanter[13]. Nominal dosage of $1x10^{17}$ ions/cm^2 of Y was implanted into the polished face of each specimen with a mean ion energy of approximately 80 keV. A 3 mm x 10 mm area near the edge of the specimen was blocked from the beam with a piece of aluminum strip to preserve an unimplanted area on each specimen. Analysis using Rutherford backscattering spectroscopy (RBS) showed that the implant had a uniform spatial distribution, a depth of about 35 nm, and an actual concentration of $5.8x10^{16}$ ions/cm^2.

Diffusion annealing of the implanted specimens was carried out at 1000°C in sealed quartz capsules. The specimen to be treated was first placed inside a small cylinder made out of tantalum foils, then put into a quartz tube which was evacuated to approximately 10^{-5} torr and filled with high purity helium prior to sealing. The Ta was used as an oxygen getter inside the capsule; otherwise the implanted Y would easily be oxidized by the residual oxygen of several hundred ppm. Since the volatility of Ta is extremely low, it was not expected to penetrate into the specimen to affect the annealing process.

Oxidation tests of implanted specimens were carried out isothermally at 1000°C for different durations. Specimens contained in an alumina boat were pushed into the hot zone of a furnace through which dry oxygen at 1 atm pressure was flowing to initiate the reaction. After the desired oxidation time, specimens were cooled in the ambient by quickly drawing the alumina boat out of the furnace. Observation and analysis of the oxide scale were made from the scale top surface as well as from its underside. To expose the underside of an adherent scale, the specimen was first mounted, then polished from the backside until only a thin layer of alloy was left. The remaining alloy was eventually etched away using 10vol% Br_2 in methanol.

Secondary ion mass spectroscopy (SIMS) analysis was used to study the distribution of Y before and after diffusion anneal and oxidation. All analyses were performed on a CAMECA IMS-3f ion microprobe. The samples were analyzed using a 4 μA, 12 kV O_2^+ primary ion beam rastered over an area of 500x500 μm^2. The smallest contrast diaphragm and a field aperture of 30 μm was used to reduce ion transmission by allowing only ions emitted from the central 30 μm diameter of the rastered area to be mass analyzed. The Y profile was quantified using a relative sensitivity factor derived from an implant standard calibrated by RBS. Depth scales were obtained by measurement of the analytical craters using an Alpha-Step stylus profilometer.

RESULTS

Effect of Y on oxidation

Oxidation kinetics of the implanted and the unimplanted Ni-25Cr at 1000°C are presented in Figure 1. The amount of oxide which spalled from the specimen surface upon cooling is also presented. Y-implantation is seen to have greatly reduced the oxide growth rate and improved the spallation resistance of the oxide scale. Both the implanted and the unimplanted specimen oxidized near parabolically, that is $x^2 = k_p t$, where x is the scale thickness, k_p is the parabolic rate constant and t is the oxidation time. From polished cross-sections of oxidized specimens, the scale thickness could be determined. The rate constant, k_p, was thus calculated to be 3.2×10^{-13} cm^2/sec for the implanted, and a factor of 10 higher for the unimplanted.

The oxide formed at early times on both the implanted and the unimplanted surfaces was identified by X-ray diffraction to be Cr_2O_3. With longer oxidation times, Ni-containing oxides began to appear as nodules on top of the Cr_2O_3 layer on the unimplanted region, but on the implanted side, the oxide remained as fine-grained Cr_2O_3. Cross sectional observations of these scales showed that neither the implanted nor the unimplanted area had any oxide pegs, but the implanted side developed a more ragged oxide which gave rise to a more tortuous scale/alloy interface[10,15].

Distribution of Y studied by SIMS

SIMS depth profiles of Y, Cr and Ni from the top surface of the oxide scale which formed on the Y-implanted area after 24h oxidation is shown in Figure 2. The Ni content was slightly higher at the outer surface. This is believed to be part of the transient oxide which formed upon initial oxidation. The scale/alloy interface was determined by measurements of the scale thickness through cross-sectioning. Yttrium is seen to be concentrated near the outer surface of the scale. However, due to the roughness of these oxide layers, depth resolution was very poor. As a result, it was impossible to determine if Y had penetrated into the alloy.

In order to determine the Y concentration in the oxide near the scale/alloy interface, SIMS depth profiles were performed from the underside of the oxide scales. Figure 3(a) shows such an analysis. The oxide which was mounted on epoxy was gold-coated to avoid charging. Very little Y was present at the underside of the oxide, but its concentration quickly rose as one sputtered inward. Since the underside of the oxide was as rough as its surface, depth resolution was again poor. Therefore, the high Y concentration near the oxide surface, which was observed when the analysis was made from the top side of the oxide, became unnoticed. In Figure 3(b), only the Y profiles close to the scale underside are presented. These profiles were normalized by fixing their Cr counts to be the same. The background level was obtained from oxides on the unimplanted region. From Figure 3(b), it is seen that within instrumental error, which is normally a factor of two of the ion counts, the level of Y at the underside of the scale can be considered to be within background counts. With the slower sputtering rate, the Y content was found to remain at the background level within a small region, about 25 nm, before rising. The rise of Y to its maximum concentration was slower in a thicker oxide. This observation is in agreement with previous studies[8-10] which concluded that the scale growth in this system is controlled by oxygen inward diffusion.

From Fig. 3(b), the concentration of Y at the scale/alloy interface in the oxide part is seen to be zero. Although this suggests that the Y concentration in the alloy must also be zero, it would still be desirable to directly analyze the underlying alloy. Figure 4 shows SIMS profiles of Y, Ni and Cr through the top surface of a 10 min oxide. In the insert is the Y profile taken at the alloy surface. It was possible to have access to the alloy surface because of some unexpected oxide loss caused by an oil vapor contamination during specimen cooling. The contamination had such a dramatic effect on scale spallation that it repeatedly caused the entire scale from an unimplanted specimen to spall off, which normally would only show negligible oxide loss. This anomalous behavior is presently being investigated. In any case, the contamination allowed the analysis of the underlying alloy to be performed, which would otherwise be impossible. A thin oxide film rich in Ni, which formed during the specimen cooling process, covered the exposed alloy surface, and all of the Y was found to be incorporated within this thin film. From here it is seen that the Y concentration in the alloy after just 10 min of oxidation at 1000°C was merely 17 ppm, and its total concentration was calculated to be only 1.8×10^{13} ions/cm^2.

Diffusion of Y in the alloy

Diffusion annealing of the implanted Y was carried out at the oxidation temperature, and Y penetration into the alloy was subsequently studied by SIMS. In none of the annealed specimens was Ta found, indicating that the Ta, which was used as an oxygen getter in the quartz capsule during annealing, did not diffuse into the alloy. Figure 5 shows the SIMS profiles of Y before and after diffusion anneals of 10min and 10h. In both the annealed cases, the surface concentration of Y was higher than expected, and this high concentration coincided with the maximum Y peak in the as-implanted state, which was about 11 at%. Much of the Y in the initial annealing state was incorporated in a thin surface oxide layer which was approximately 0.2 μm thick. However, after longer annealing times, one hour and up, this surface oxide no longer existed. It seems reasonable that initially, the Y-implanted surface reacted

faster than the Ta foil with residual oxygen in the quartz capsule. With time, this surface oxide became reduced by the Ta, which forms thermodynamically more stable oxides than Y, Ni or Cr. Since only 10.53 at% of Y is necessary to completely form Y_2Ni_{17}, and the solubility limit of Y is less than 1 at% in Cr_2O_3-forming Ni alloys[14], the high surface concentration of the annealed sample after longer oxidation times could be due to the formation of second phase particles. For example, $Y_2(Fe,Cr)_{17}$ particles have been found in a Fe-Cr alloy implanted with Y by King and Grabowski[8]. Whether the surface Y was tied up into an initial oxide or in Y-Ni intermetallic particles, some Y must have diffused into the alloy as seen from the tails of these SIMS profiles. To estimate a diffusivity from this Y penetration, a thin film solution of Fick's second law was used where C(x,t) is proportional to $\exp(-(x-x')^2/4Dt$; x' is taken as the maximum Y concentration of the as-implanted sample. The diffusivity thus calculated from several different diffusion times was $(2.6\pm1.3)\times10^{-13}$ cm^2/sec.

DISCUSSION

Ion-implantation of 5.8×10^{16} ions/cm^2 of yttrium in Ni-25Cr produced a maximum Y concentration of nearly 11 at% which is well over its solubility limit in the alloy[14]. Upon heating to high temperatures, some of this Y is expected to form Y_2Ni_{17} particles with the substrate. However, due to its high affinity for oxygen, most of this Y quickly became incorporated into a thin surface oxide layer under even a few ppm of oxygen. The diffusivity of ion-implanted Y into the alloy calculated from this study is about 2.6×10^{-13} cm^2/sec. This value is comparable to the oxidation rate of the implanted surfaces, which is 3.2×10^{-13} cm^2/sec. From these values alone, one would not expect a lot of the implanted Y to remain in the alloy under a highly oxidizing environment.

Indeed, after only 10 minutes of oxidation at 1000°C, the amount of Y left in the alloy was found to be 17 ppm, or 11 ppm by weight, with a total concentration of about 2×10^{13} ions/cm^2. Furthermore, all of this Y is concentrated near the

scale/alloy interface, instead of being diffused a long way back into the alloy. It is well established that the steady state oxide growth of these high-dose Y-implanted specimens is via oxygen inward transport[8-10]. As oxidation continues, the oxide thickens at the scale/alloy interface, and this growth process is expected to incorporate the remaining Y into the oxide scale. After 24 hours of oxidation, SIMS analyses from the underside of the oxide scale showed that the Y concentration at the scale/alloy interface in the oxide part is zero within experimental errors. Nevertheless, the resulting oxide scale was still extremely adherent.

From these results, it is clear that the continued presence of reactive elements in the alloy is not essential for better Cr_2O_3 scale adhesion. There is definitely not enough Y to form large numbers of Y_2O_3 particles in the alloy to assist oxide peg formation. Furthermore, previous studies of these Y-implanted specimens have shown that the scales developed no pegs, yet they were adherent[10,15]. The vacancy sink model is equally unlikely for the same reason that there is no Y left in the alloy to trap the vacancies to keep them from condensing at the interface.

The starting Ni-25Cr alloy had about 51 ppm of sulfur as an intrinsic impurity. It is very likely that the implanted Y can getter sulfur which diffuses to the alloy surface upon initial heating of the alloy. A previous SIMS study by Hou and Stringer[15] did show a small sulfur peak in the Cr_2O_3 scale, and its location coincided with the maximum Y content in the oxide. Although sulfur diffusion, 1.56×10^{-9} cm^2/sec at 1000°C in Ni[16], is much faster than the oxide growth rate or the Y diffusion rate, its segregation is eventually limited by surface coverage. The saturation coverage of sulfur on Ni is at 1/2 a monolayer[17], which amounts to about 10^{15} atoms/cm^2. The initial scavenging then, would only take away a small fraction of the sulfur impurity. Results from this study showed that the implanted Y which is left in the alloy after 10 minute oxidation was only of the order of 10^{13} ions/cm^2. Implantation of less than 1×10^{16} ions/cm^2 is not even enough to produce an adherent oxide scale with this alloy[7], the small remaining amount definitely cannot trap enough

sulfur to provide a strong interface. This indicates that the sulfur gettering mechanism is also not of importance for Cr_2O_3-forming alloys. Rather, the good scale adhesion may be a result of the modified oxide growth which is provided by the presence of yttrium in the oxide.

CONCLUSIONS

High dose ion-implantation of yttrium in Ni-25Cr alloy reduced the alloy's oxidation rate at 1000°C by one order of magnitude and greatly improved the spallation resistance of the Cr_2O_3 scale which formed. The implanted yttrium quickly became incorporated within the oxide scale. After 10 minutes of oxidation, only 17 ppm, or 2×10^{13} ions/cm^2, of yttrium was left in the alloy. With further oxidation, the implanted yttrium remained concentrated near the oxide surface as the oxide thickened with time. Within the oxide layer, the yttrium concentration progressively dropped to zero at the scale/alloy interface. Diffusivity of the implanted yttrium in the alloy was estimated to be 2.6×10^{-13} cm^2/sec at 1000°C. Based on these results, it was concluded that none of the implanted yttrium would be left in the alloy after a few hours of oxidation. Therefore, those mechanistic models which require the presence of reactive elements in the alloy, either to act as a sink or to provide fast diffusion paths, cannot be responsible for the improved adhesion found with reactive element additions in Cr_2O_3-forming alloys.

ACKNOWLEDGEMENT

The authors would like to thank Mrs. Z. R. Shui for carrying out most of the sample preparations. This work was supported by the Electric Power Institute under contract No. RP 2261-1, through an agreement with the U. S. Department of Energy under Contract No. DE-AC03-76SF00098.

REFERENCES

1. L. B. Pfeil, 1937 U. K. Patent No. 459848.
2. D. P. Whittle, and J. Stringer, Phil. Trans. Roy. Soc. London, A27(56) (1979) 309.

3. M. J. Bennett, High Temperature Corrosion, NACE, 6 (1983) 145.

4. A. Galerie, M. Caillet and M. Pons, Mat. Sci. and Eng., 69 (1985) 329.

5. G. Dearnaley, Nucl. Instrum. Methods, 182/183 (1981) 899.

6. J. C. Pivin, C. Roques-Carmes, J. Chaumont and H. Bernas, Corr. Sci, 20 (1980) 947.

7. Peggy Y. Hou, Ph.D. Thesis, Material Science Dept., UC Berkeley, (1986).

8. W. E. King and K. S. Grabowski, in G. S. Was and K. S. Grabowski (ed.), Environmental Degradation of Ion and Laser Beam Treated Surfaces, TMS publication, 1989, p. 277.

9. C. M. Cotell, G. J. Yurek, R. J. Hussey, D. F. Mitchell and M. J. Graham, J. Electrochem. Soc., 134 (1987) 1871.

10. P. Y. Hou, I. G. Brown and J. Stringer, paper presented at the 7th International Sym. on Ion Beam Modification of Materials, Knoxville, Tenn., Sept. 9-14, 1990, to be published in Nuclear Instruments and Methods, Sec. B.

11. A. W. Funkenbusch, J. G. Smeggil and N. S. Bornstein, Metll. Trans., 16A (1985) 1164.

12. R. A. Collins, S. Muhl and G. Dearnaley, J. Phys F: Metal Phys., 9 (1979) 1245.

13. I. G. Brown, M. R. Dickinson, J. E. Galvin, X, Godechot and R. A. MacGill, paper presented at this conference.

14. R. P. Elliot, Constitution of Binary Alloys, First Supplement, McGraw-Hill, New York, 1965, p. 366.

15. P. Y. Hou and J. Stringer, Oxid. of Metals, 34 (1990) 299.

16. T. Kiyahara, K. Stolt, D. A. Reed, H, K. Birnbaum, Scripta Met., 19 (1985) 117.

17. P. Marcus and J. Oudar, in E. McCafferty, C. R. Clayton, J. Oudar (ed.), Fund. Aspects Cor. Prot. by Surf. Mod., Proc. Electrochem. Soc., (1984) 173.

FIGURE CAPTIONS

Figure 1: Oxidation kinetics at 1000°C in 1 bar oxygen for the unimplanted and the Y-implanted Ni-25Cr. The actual implantation dosage was 5.8×10^{16} ions/cm^2. The amount of oxide which spontaneously spalled off from the specimen surface during cooling is also included.

Figure 2: SIMS depth profiles of Y, Cr and Ni through the surface of a 24 hour oxide. The location of the scale/alloy interface was obtained from cross-sectioning the oxidized specimen.

Figure 3: (a) SIMS depth profiles of Y, Cr and Ni through the underside of a 24 hour oxide. The oxide was mounted in epoxy with the substrate first thinned on SiC paper, then chemically etched using Br_2/MeOH. (b) Comparison of Y profiles near the scale underside of two oxides, 24h and 50h, and with two sputtering rates. The slow rate is 1/8 that of the fast one.

Figure 4: SIMS depth profiles of Y, Cr and Ni through the surface of a 10 minute oxide. In the insert is shown the profile of Y within the underlying alloy.

Figure 5: SIMS depth profiles of yttrium in the as-implanted sample and in samples which have gone through diffusion anneals at 1000°C for two different durations.

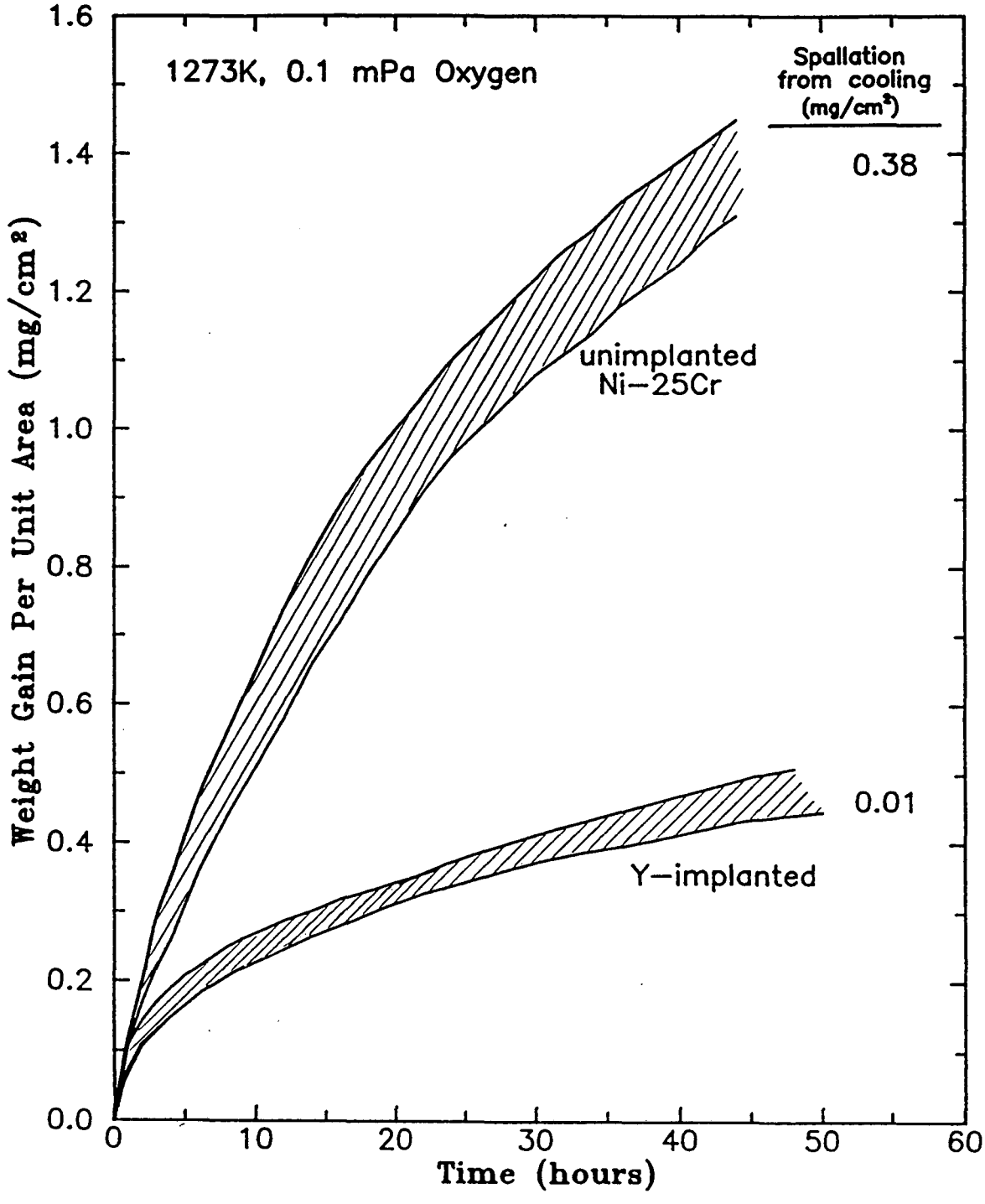
1273K, 0.1 mPa Oxygen
Spallation from cooling (mg/cm²)
0.38
0.01
unimplanted Ni–25Cr
Y–implanted
Weight Gain Per Unit Area (mg/cm²)
Time (hours)
0.0
0.2
0.4
0.6
0.8
1.0
1.2
1.4
1.6
0
10
20
30
40
50
60

Figure 1

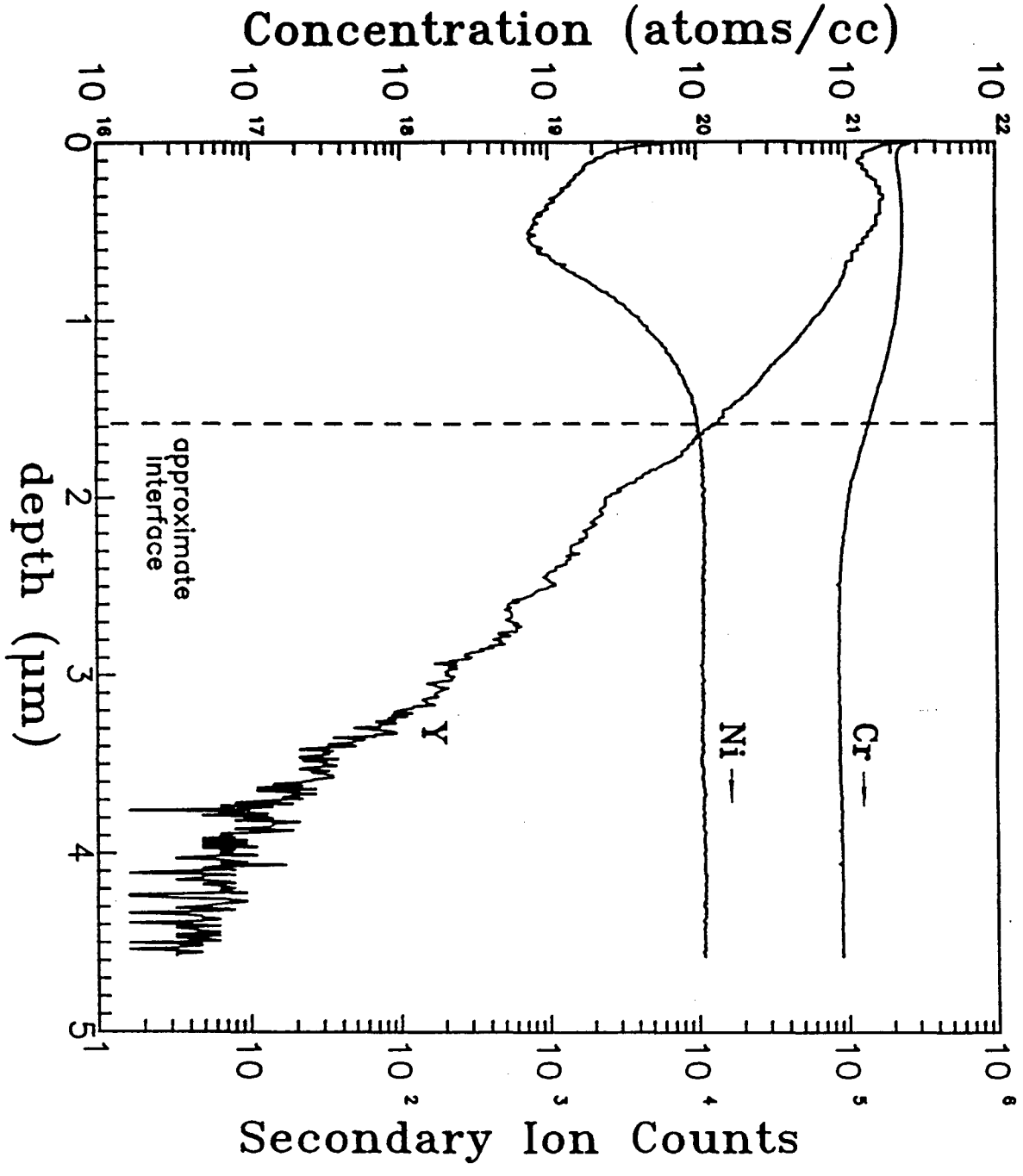
Concentration (atoms/cc)
10 22
10 21
10 20
10 19
10 18
10 17
10 16
Cr
Ni
Y
approximate interface
depth (µm)
0
1
2
3
4
5
Secondary Ion Counts
10 6
10 5
10 4
10 3
10 2
10
1

Figure 2

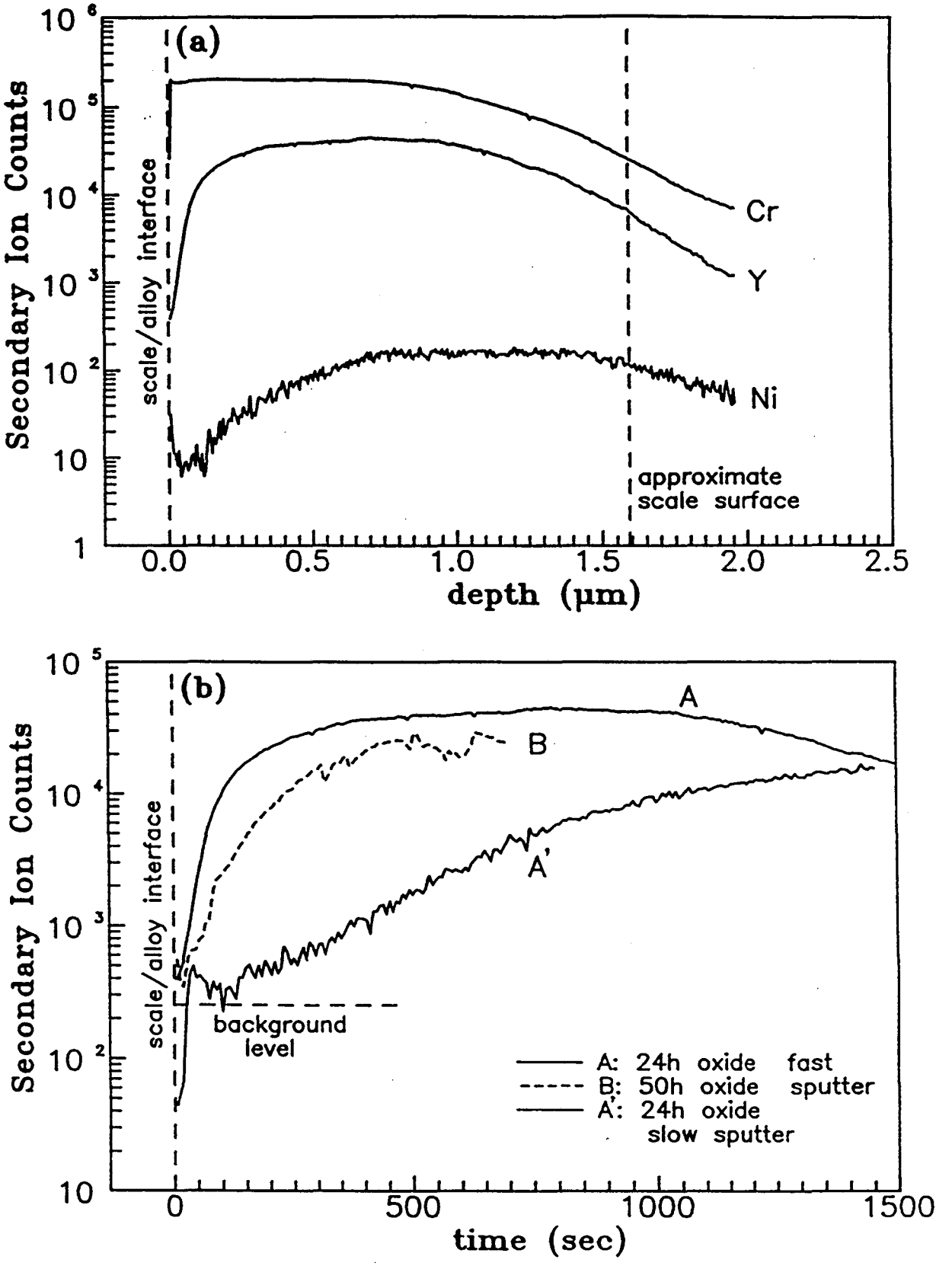
(a)
Secondary Ion Counts
scale/alloy interface
Cr
Y
Ni
approximate
scale surface
depth (µm)
(b)
A
B
A'
background
level
A: 24h oxide fast
B: 50h oxide sputter
A': 24h oxide
slow sputter
time (sec)

Figure 3

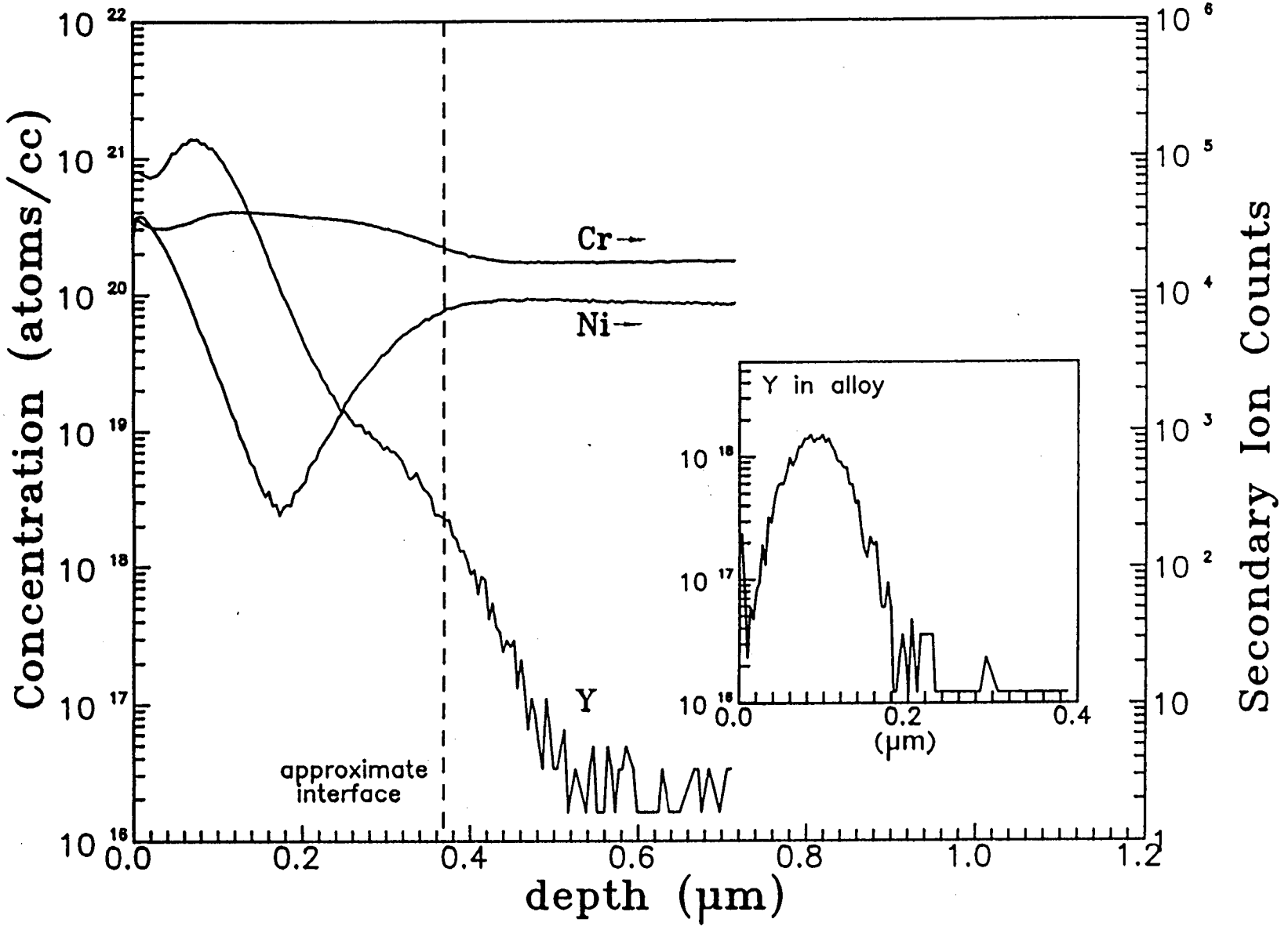
Concentration (atoms/cc)
Secondary Ion Counts
depth (μm)
Cr
Ni
Y
approximate interface
Y in alloy
(μm)

Figure 4

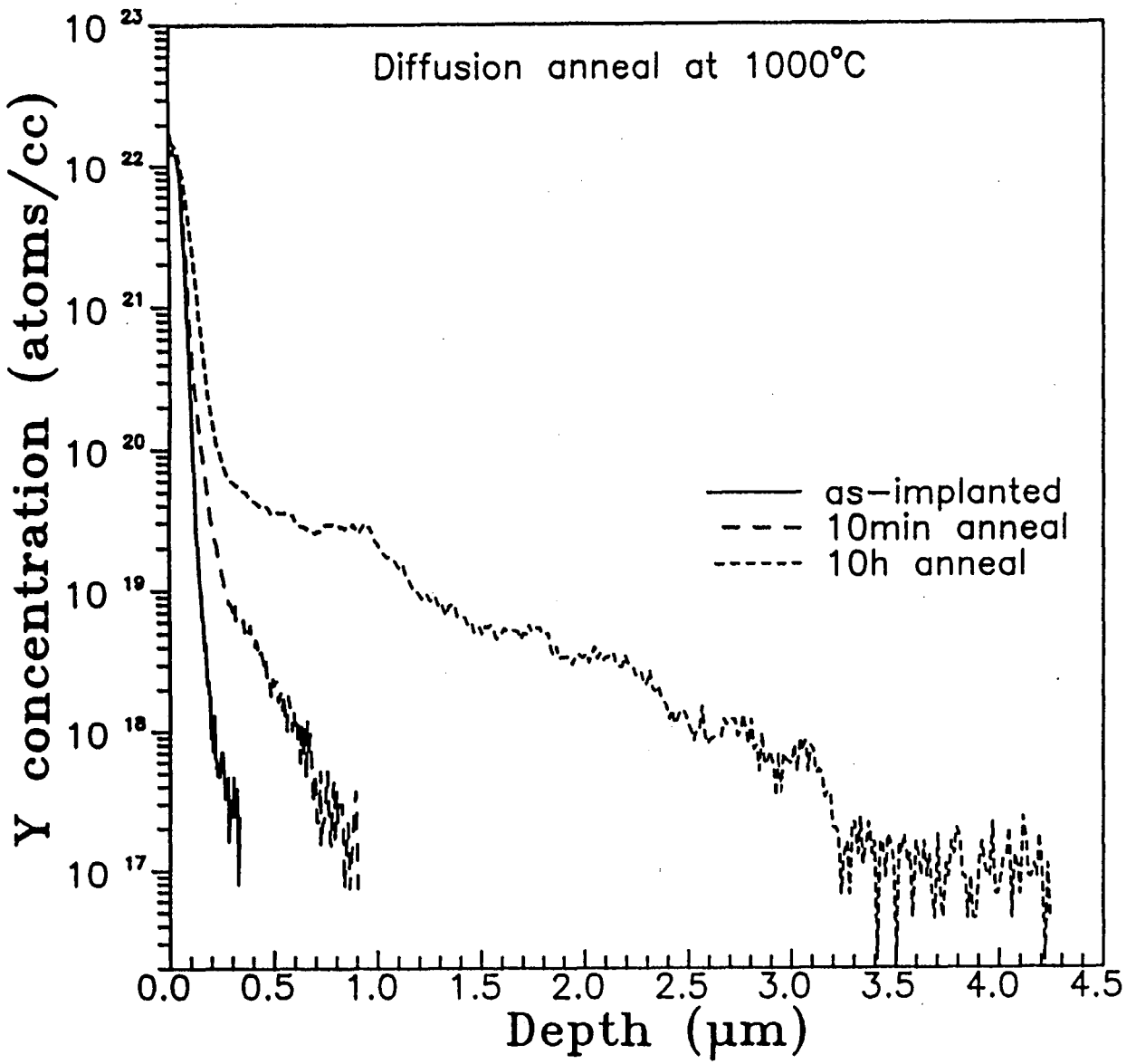
Diffusion anneal at 1000°C
as-implanted
10min anneal
10h anneal
Y concentration (atoms/cc)
10 23
10 22
10 21
10 20
10 19
10 18
10 17
0.0
0.5
1.0
1.5
2.0
2.5
3.0
3.5
4.0
4.5
Depth (µm)

Figure 5

LAWRENCE BERKELEY LABORATORY
UNIVERSITY OF CALIFORNIA
INFORMATION RESOURCES DEPARTMENT
BERKELEY, CALIFORNIA 94720